

Temperature-Dependent Structure–Energy Changes in Crystals of Compounds with Poly(hydroxymethyl) Grouping

N. I. Golovina,¹ A. V. Raevskii, B. S. Fedorov, N. V. Chukanov, G. V. Shilov,
L. S. Leonova, V. P. Tarasov, and L. N. Erofeev

Institute of Problems of Chemical Physics, Russian Academy of Sciences, 142432 Chernogolovka, Moscow Region, Russian Federation

Received July 31, 2001; in revised form November 14, 2001; accepted December 3, 2001

Crystals of tris(hydroxymethyl)nitromethane (**1**) and tris(hydroxymethyl)aminomethane (**2**) were prepared and grown at room temperature. X-ray analysis was used to study the structure of crystals **1** and **2** at room temperature; the X-ray diffraction method was applied to investigate polycrystalline samples during a temperature rise up to the phase transition into the plastic phase. Phase transitions in separate crystals **1** and **2** were observed in a hot stage under an optical microscope. Calorimetric study of the crystal temperature behavior and the phase transition features including melting were carried out. By IR spectroscopy the temperature relations of the bonds of symmetric N–O stretching vibrations of nitro groups and stretching vibrations of OH groups redistribution in crystals of **1** were investigated. In crystals of **2** the behavior of stretching vibration bands of O–H groups was studied at room temperature. In the temperature interval including phase transition, data on structure–dynamic rearrangements in the crystal lattice of compounds **1** and **2** were obtained by the NMR pulse method in the solid phase using relaxational free induction decay of protons. The proton conductivity was found and its temperature parameters were determined for both compounds in the plastic state. © 2002 Elsevier Science (USA)

INTRODUCTION

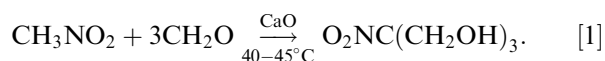
A complex study of structure–energy changes both in separate molecules and in a crystal lattice as a whole for the compounds $RNO_2C(CH_2OH)_2$, where $R = Br, NO_2$, was carried out in our earlier work [1–3]. It has been shown that conformational changes in the molecules during temperature elevation begin from torsional oscillations in the most energy-consuming fragments, nitro groups, and are accompanied by the redistribution of structure, forming hydrogen bonds. In this case the phase transitions are only a part of

this multifactor process. IR spectra demonstrate that the barrier for torsional vibrations of a nitro group in the molecules with $R = Br$ is 2.7 kcal/mol and in the molecules with $R = NO_2$ the barrier is about 3.8 kcal/mol. The barrier in a molecule consists of steric obstacles to nitro group vibrations and of the energy-stabilizing molecular conformation comprising orbital and electrostatic interactions. As the barriers are essential to the temperature-dependent changes in the crystal lattice and, first of all, during conformational transitions in separate molecules, it was of interest to investigate the compounds having lower barriers to torsional movement in a molecule. For that, compounds of $RC(CH_2OH)_3$ type were chosen, where $R = NO_2, NH_2, CH_2OH$. The structures of the compounds were obtained earlier (4–6).

The presented work deals with the re-study of the structure of the compounds by different physical methods regarding temperature dynamics of the crystal lattice, peculiarities of phase transformations, and the construction details of intermediate phases. The final cubic phase—the last solid state phase of the crystals (the plastic state)—with total rotation of molecules in the crystal structure and with occurrence of ion (proton) conductivity is also of considerable interest. In the present work the method of direct measurement of conductivity was added to the techniques we used earlier: X-ray analysis, IR spectroscopy, calorimetry, pulse NMR (in the solid phase), and optical microscopy. In this respect the work is an extended continuation of the previous trend of our investigations.

EXPERIMENTAL

Tris(hydroxymethyl)nitromethane (**1**) was prepared from nitromethane and formaldehyde in the presence of CaO at 313–318 K:



¹To whom correspondence should be addressed. Fax: (096)5153588. E-mail: niv@icp.ac.ru.

The crystals **1** for investigation were grown from a mixture of isopropyl alcohol and chloroform. Tris(hydroxymethyl)aminomethane (**2**) was prepared by reduction of **1** on Zn in the presence of HCl,



and the crystals (**2**) were grown from ethanol solution.

1. X-Ray Study

The structure of tris(hydroxymethyl)nitromethane (**1**) and tris(hydroxymethyl)aminomethane (**2**) was studied at

room temperature. The reflection intensities were measured in the range $0.02 \leq \sin \theta / \lambda \leq 0.50$ on a four-circle KM-4 (KUMA-Diffraction, Poland) diffractometer with the $\omega/2\theta$ scanning technique. The total number of independent reflections was 1449 for structure **1** and 707 for structure **2**. Crystals **1** are triclinic with the following parameters: $M = 151.12$, $a = 9.820(2) \text{ \AA}$, $b = 6.105(2) \text{ \AA}$, $c = 6.219(3) \text{ \AA}$, $\alpha = 109.61(3)^\circ$, $\beta = 89.84(3)^\circ$, $\gamma = 109.61(3)^\circ$, $V = 351.06(9) \text{ \AA}^3$, $d = 1.428(8) \text{ g/cm}^3$, $\lambda K\alpha = 1.5418 \text{ \AA}$, space group $P1$, $Z = 2$, $\mu = 1.173 \text{ mm}^{-1}$.

Crystals of **2** are rhombic: $M = 121.14$, $a = 8.850(3) \text{ \AA}$, $b = 8.802(5) \text{ \AA}$, $c = 7.807(9) \text{ \AA}$, $V = 608.20(7) \text{ \AA}^3$, $d = 1.322(9) \text{ g/cm}^3$, $\lambda K\alpha = 1.5418 \text{ \AA}$, space group $Pna2(1)$, $Z = 4$, $\mu = 1.354 \text{ mm}^{-1}$.

The structures were solved by a direct method using the SHELX-97 program on a PC. The atomic coordinates (Tables 1 and 2) in structures **1** and **2** were refined by a full-matrix approximation. The refinement for non hydrogen atoms was made in an anisotropic approximation. Hydrogen atoms were determined on a geometric model and their final position was stated according to the energy maximum of intermolecular hydrogen bonds. For 1057 reflections having $F_o > 4\sigma(F_o)$ in the structure **1**, $R = 0.064$, and for 629 reflections with $F_o > 4\sigma(F_o)$ in the structure **2**, $R = 0.074$. Two crystallographically independent molecules with different conformations (Fig. 1) are in the unit cell of the triclinic noncentrosymmetrical crystal **1**. $\text{CH}_2\text{-OH}$ groups in both molecules are positioned round the local

TABLE 1

Atomic Coordinates ($\times 10^4$) and Equivalent Isotropic Displacement Parameters ($\text{\AA}^2 \times 10^3$) for Structure **1**, $\text{C}_4\text{H}_9\text{NO}_5$ (U_{eq} Is Defined as One-Third of the Trace of the Orthogonalized U_{ij} Tensor)

Atom	X	Y	Z	U_{eq}
O(1)	65(15)	7341(3)	1002(17)	146(6)
O(2)	1989(12)	8637(5)	1361(2)	211(10)
O(3)	-423(6)	4407(9)	3717(9)	66(2)
O(4)	3586(5)	7368(10)	4876(8)	62(2)
O(5)	273(6)	1728(8)	6077(9)	63(2)
O(6)	6732(11)	295(19)	-4436(12)	107(4)
O(7)	5426(20)	3053(20)	-3545(16)	166(11)
O(8)	8706(5)	1982(10)	-441(8)	66(2)
O(9)	4969(5)	5553(9)	1140(8)	60(1)
O(10)	4986(6)	-1750(9)	-1310(9)	59(2)
N(1)	1128(7)	7852(12)	2075(10)	64(2)
N(2)	6205(7)	1862(10)	-3005(9)	57(2)
C(1)	1136(6)	7792(10)	4522(8)	43(1)
C(2)	-254(7)	6809(13)	4981(11)	54(2)
C(3)	2298(7)	6234(12)	4769(11)	54(2)
C(4)	1373(7)	10292(12)	6133(13)	54(2)
C(5)	6222(6)	1981(9)	-498(8)	42(1)
C(6)	7499(7)	779(11)	-112(10)	49(2)
C(7)	6237(7)	4507(10)	1077(10)	52(2)
C(8)	4942(6)	678(11)	-139(11)	51(2)
H(1)	-735(160)	4242(150)	2396(140)	120(20)
H(2)	4011(90)	6739(160)	3638(160)	70(20)
H(3)	-252(100)	11838(180)	7195(170)	60(20)
H(4)	-968(120)	7645(150)	4579(150)	90(20)
H(5)	-329(60)	7035(100)	6581(110)	40(20)
H(6)	2273(100)	4812(170)	3492(180)	80(20)
H(7)	2163(90)	5849(160)	6131(160)	60(20)
H(8)	2195(100)	10927(170)	5707(170)	50(20)
H(9)	1491(90)	10285(140)	7662(150)	50(20)
H(10)	8946(150)	1435(160)	-1829(150)	120(20)
H(11)	4683(130)	6658(180)	355(180)	100(20)
H(12)	4976(170)	-2464(180)	-349(180)	140(20)
H(13)	7492(120)	-790(180)	-1156(180)	90(20)
H(14)	7495(100)	724(170)	1412(170)	90(20)
H(15)	6479(80)	4573(150)	2593(140)	90(20)
H(16)	6922(70)	5374(130)	570(120)	100(20)
H(17)	4164(110)	1279(180)	-661(120)	100(20)
H(18)	4833(80)	950(140)	1463(180)	90(20)

TABLE 2

Atomic Coordinate ($\times 10^4$) and Equivalent Isotropic Displacement Parameters ($\text{\AA}^2 \times 10^3$) for Structure **2**, $\text{C}_4\text{H}_{11}\text{NO}_3$ (U_{eq} Is Defined as One-Third of the Trace of the Orthogonalized U_{ij} Tensor)

Atom	X	Y	Z	U_{eq}
O(2)	-4569(3)	-777(4)	1443(7)	63(1)
O(3)	-2678(4)	-179(5)	-2444(5)	55(1)
O(4)	628(3)	309(4)	72(4)	43(1)
N(1)	-1496(4)	-1385(4)	1954(5)	39(1)
C(1)	-2010(4)	-316(4)	611(5)	31(1)
C(2)	-3479(4)	388(4)	1192(6)	40(1)
C(3)	-2217(4)	-1176(5)	-1080(5)	40(1)
C(4)	-827(4)	942(4)	431(6)	37(1)
H(1)	-2350(100)	-2175(100)	2741(150)	100(70)
H(2)	-4387(150)	-1526(200)	1925(110)	100(40)
H(3)	-2576(200)	737(150)	-2137(200)	240(90)
H(4)	642(170)	-609(150)	351(200)	260(60)
H(5)	-3337(110)	936(90)	2225(130)	50(20)
H(6)	-3857(80)	1097(70)	336(90)	50(14)
H(7)	-2942(70)	-1960(60)	-954(90)	59(14)
H(8)	-1263(100)	-1640(80)	-1401(110)	70(20)
H(9)	-1127(70)	1629(60)	-504(80)	46(14)
H(10)	-786(50)	1525(50)	1442(100)	42(10)
H(11)	-399(150)	-191(140)	702(110)	52(10)

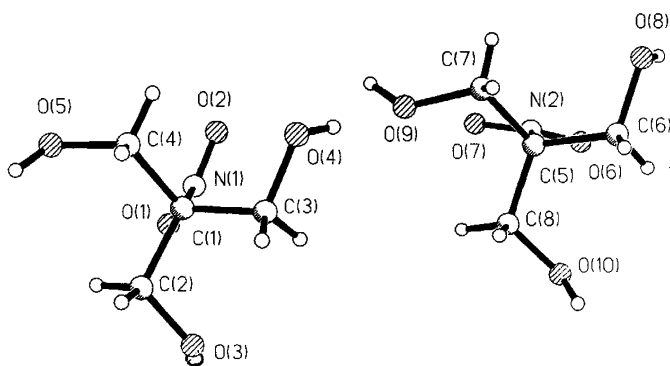


FIG. 1. Molecules of tris(hydroxymethyl)nitromethane **1**.

axis of the third order directed along the C–N bond. Stabilization of both molecules in structure **1** is created by a weak orbital interaction with probable donation of electron density from the π_Z -populated orbital of a nitro group into the vacant one— $\sigma^*(C-O)$ —the orbital of the polar C–O bond. The energy of such interaction is not great, no more than 1.5 kcal/mol. The conformations of the two independent molecules are slightly different; the angle between the normal to the plane C(1)N(1)O(1)O(2) and the line C(2)O(3) in a molecule of one type constitutes 27.7° , and the angle in the molecule of the other type is 15.5° . It is the construction which predetermines the π_Z - σ^* orbital interaction donating electron density into the orbital of the $C^{+\delta}-O^{-\delta}$ bond. It is evident that the orbital interactions in the other molecule will be stronger. The nitro group easily

overcomes the barrier with the help of torsional vibrations and can interact with the next C–O bond, which is a new electron “trap” in this case. Note that oxygen atoms of the nitro groups have the greatest thermal vibrations in comparison to other atoms and the major axes of the thermal vibration ellipsoids are orthogonal to the nitro group planes. Projection (ac) of the crystal **1** structure (Fig. 2) at room temperature demonstrates the structure of a body-centered cube (bcc) in the vertices of which molecules of the one type are located, in the center of the cube molecules of the other type are positioned. In the structure short intermolecular contacts between oxygen atoms of neighboring molecules are noticeable with the values

$$\begin{aligned} O(3) \cdots O(5) &= 2.642 \text{ \AA}, O(3) \cdots O(8) = 2.642 \text{ \AA}, \\ O(4) \cdots O(9) &= 2.610 \text{ \AA}, O(4) \cdots O(10) = 2.631 \text{ \AA}, \\ O(5) \cdots O(8) &= 2.617 \text{ \AA}, O(9) \cdots O(10) = 2.591 \text{ \AA}. \end{aligned}$$

However, the mentioned short contacts between oxygen atoms of hydroxyl groups do not at all mean the existence of strong hydrogen bonds between the molecules. The calculations of structure energy by the atom–atom potential method taking into account the energy of the hydrogen bond using the MMX (7) program give the following: dispersion energy is -8.806 kcal/mol and the energy of the intermolecular hydrogen bonds is -1.5 kcal/mol.

The unit cell of rhombic crystal **2** with $Z = 4$ in general position has only one crystallographically independent molecule. The molecule **2** is asymmetric and has no local elements of symmetry (Fig. 3). Projection (ab) of crystal **2** structure (Fig. 4) also demonstrates this type of body-centered cube (bcc). In other words, the structures **1** and **2** have preparations of cubic phase. In the structure **2** short contacts are noticeable between oxygen atoms of hydroxyl groups with the following values: $O(2) \cdots O(5) = 2.729 \text{ \AA}$, $O(3) \cdots O(4) = 2.675 \text{ \AA}$. Calculations of energy for structure **2** by the atom–atom potential method taking into account hydrogen bond energy using the MMX (7) program produce the following values: dispersion energy is -8.580 kcal/mol and the energy of the intermolecular hydrogen bonds is -0.963 kcal/mol.

2. Temperature X-Ray Diffraction Study

The temperature X-ray diffraction study of the single crystals **1** and **2** turned out to be impossible as the crystals partially desintegrated during a temperature rise. To perform the study, polycrystal samples were used, placed in the variable-temperature cell of a DRON-M diffractometer (temperature accuracy ± 1 K). The pulse counting was done at a rate of 2 K/min. Theoretical powder patterns were previously calculated using the results of the

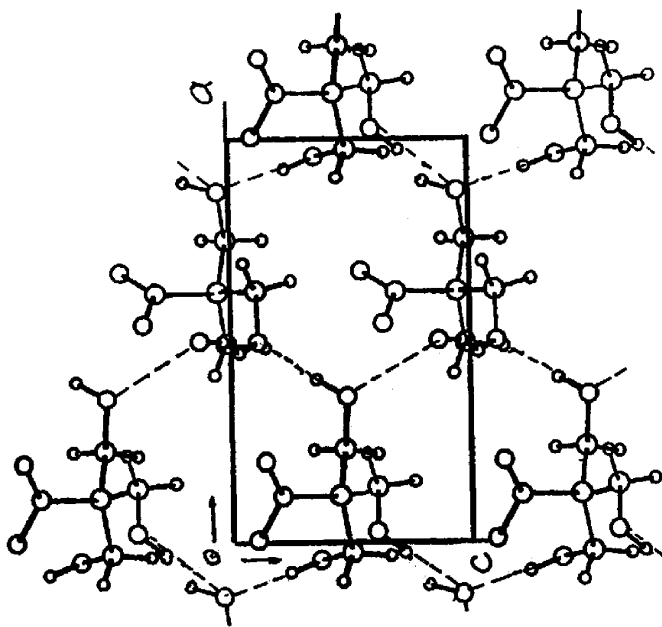


FIG. 2. Projection of the structure **1** on plane (ac).

TABLE 4
Diffraction of Polycrystals 2 at $T = 293$ K and $T = 410$ K

(D) $T = 293$ K					(E) $T = 410$ K				
NN	$2\theta^\circ$	I_R	d (Å)	hkl	NN	$2\theta^\circ$	I_R	d (Å)	hkl
1	14.7	20	6.07		1	14.7	6	6.017	
2	18.6	60	4.754		2	18.7	>100	4.754	110
3	20.7	>100	4.279		3	23.5	3	3.775	
4	22.9	>100	3.890		4	26.4	6	3.378	200
5	25.8	18	3.454		5	28.8	3	3.093	
6	27.4	7	3.263		6	31.4	12	2.842	211
7	29.0	3	3.081		7	36.4	5	2.468	
8	31.0	60	2.884						
9	31.6	45	2.831						
10	34.5	23	2.602						
11	36.5	12	2.460						
12	37.3	8	2.414						
13	37.8	6	2.384						
14	39.0	50	2.313						
15	40.2	6	2.245						

volume (to its decrease) and results in a decrease of the parameter a (6.898 Å as compared to 6.936 Å).

Diffraction patterns of crystals **2** recorded at $T = 293$ K, $T = 410$ K, $T = 416$ K, and $T = 423$ K (Tables 4 and 5) after the phase transition ($T = 409$ K) also disclose the lattice of a body-centered cube (bcc) with parameters $a = 6.813$ Å at $T = 410$ K, $a = 6.823$ Å at $T = 416$ K, and $a = 6.845$ Å at $T = 423$ K (estimation error is 3.5%). In the plastic phase of the crystal **2** a tendency toward an increase of the cube parameter is observed. So in both structures one can find the phase transition from the crystalline state into the state of the plastic phase of a crystal when molecules lose their individuality and transform into spheroids, making definite

rotations around the gravity centre in such a way that the diffraction pattern might correspond to a ball model of the structure having body-centered cube (bcc).

3. Microscopic Observations of the Temperature Behavior of the Crystals

The Crystal 1

The study was made in a hot stage under an optical microscope (NU-2 instrument, Karl Zeiss, Jena) in polarized light with a constant heating rate of 1 K/min. The temperature accuracy was ± 1 K. Low quality of the crystals and a deposit of sublimated material on the crystal surface and on both cover glasses prevented good microphotography production. The initial crystals were colorless, defective needles, 10–15 mm long and having thickness from several to 100 μm . Growth defects were located along the longitudinal axis and produced a picture of long fibers forming the crystal. The crystals had a very rough surface. They were optically active; therefore, the phase transition into the cubic phase was convenient to observe in polarized light. Two sequences of experiments were performed in the first the observation was made with no immersion, in the air, and in the second, crystals were placed in immersion (silicon) oil.

Observations without immersion. No noticeable change in the crystals took place during the heating from room temperature to 306 K. From 306 to 340 K a volatile product condensed on a protecting glass. Above 340 K the process stopped. Near 353 K the phase transition into the cubic phase occurred and the crystals lost their optical activity. The phase transition proceeded simultaneously in all crystals as a reaction wave spreading from crystal ends

TABLE 5
Diffraction of Polycrystals 2 at $T = 416$ K and $T = 423$ K

(F) $T = 416$ K					(G) $T = 423$ K				
NN	$2\theta^\circ$	I_R	d (Å)	hkl	NN	$2\theta^\circ$	I_R	d (Å)	hkl
1	16.9	3	5.239		1	13.2	4	6.756	
2	18.7	>100	4.754	110	2	15.6	3	5.705	
3	26.3	6	3.393	200	3	18.6	40	4.784	110
4	28.8	3	3.105		4	20.3	2	4.376	
5	31.4	11	2.842	211	5	22.7	3	3.929	
6	36.4	4	2.468		6	26.3	6	3.393	200
					7	27.0	3	3.305	
					8	28.8	5	3.105	
					9	30.7	2	2.917	
					10	31.4	14	2.852	211
					11	32.2	4	2.780	
					12	34.0	2	2.637	
					13	35.0	2	2.567	
					14	35.5	2	2.525	
					15	36.5	6	2.460	

by a front zone about $20\ \mu\text{m}$ wide at a great speed. In the conversion wave front a gradient of optical activity change to its complete disappearance was seen. The fact pointed to the emergence of either an intermediate phase or nuclei of the new (cubic) phase in the bulk of the parent phase. At the temperature near 360 K traces of liquid phase started to appear, probably due to eutectics formation between the decomposition products and the initial substance. The quantity of liquid phase grew with the temperature rise. Near 373 K a part of the initial crystals maintained their solid phase while the decomposition in the liquid phase began, accompanied by gas evolution. At about 300 K only a brown liquid phase remained with slow gas liberation and observation was stopped. Thus, it has been shown that

(1) a considerable amount of volatile product is present in the sample, probably solvent traces absorbed during preparation of the substance,

(2) the substance does not have a melting point,

(3) phase transition proceeds at about 352 K from an optically anisotropic phase into an isotropic one (cubic), and

(4) pyrolysis of the compound starts in the solid phase at around the phase transition point.

Observations using immersion. To obtain better conditions for examination, the crystals were placed in a drop of immersion oil between two cover glasses. As the picture of the process in immersion totally represented the observations without immersion, particular attention was paid to the phenomenon of repeated phase transition with several runs of heating and cooling in the temperature range of direct and reverse phase transitions.

To do this, the temperature was raised several degrees (358 K) above the temperature of the direct phase transition (352 K) and later on the temperature was lowered at rate of 1 K/min until the crystal returned to the initial anisotropic phase. In the experiment the temperatures of the reverse phase transition and the crystal state were registered, and the heating and cooling cycles were repeated several times.

After six runs the crystals looked damaged; they had a great number of internal bubbles, both separated and coalesced as prolonged cavities, and sites of yellowed material. The fact could be explained by the process of thermal decomposition, that accompanied the cycles of phase transformations.

It has been found that the accumulation of decomposition products decreases the temperature point of the direct phase transition by 2 K and the temperature of the reverse phase transition by 21 K. The observed variation of the phase transition temperatures in different crystals may be explained by the dissimilar depths of the thermal

decomposition acquired by the crystals after several runs of heating and cooling. One may conclude that the introduction of impurity defects (in our case, decomposition products) into the crystal lattice decreases the temperature of the direct transition and enlarges the temperature interval of the cubic phase existence.

The Crystal 2

The initial crystals were tens of micrometers in transverse and hundreds of micrometer in longitudinal directions. They were colorless, were optically active with rotational dispersion, and contained a considerable number of growth defects. Up to 333 K no change in the crystals took place. Starting from 333 K and higher, one could see an intensive formation of small drops of condensation on a protecting glass, which probably is connected with the evolution of solvent adsorbed on growth defects and micropores. As the temperature increased, the condensation evolution gradually decreased and at 353 K came to an end. At 400 K phase transition from an anisotropic phase into a cubic (isotropic) one occurred, resulting in the loss of optical activity of the crystals. The phase transition developed simultaneously in all crystals, spreading in the form of a narrow front of the interface boundary. One could see in the crystals of cubic modification transparent optically active intrusions of crystalline particles $2\text{--}10\ \mu\text{m}$ in diameter constituting 2–3% of the total mass. (Later on, the particles stayed during all stages of conversions. This might be explained by technological impurities formed during the preparation or present in the parent reagents). At 423 K a real melting of cubic phase crystals took place and a thin, optically passive film was formed on a glass holder. Then the temperature was raised to 450 K but no noticeable changes occurred. During the temperature fall the liquid phase turned into a solid film of cubic phase at 425 K, that is, almost without overcooling. The cubic phase film being continuous at first, started cracking when the temperature decreased, which was probably connected with the decrease of the phase volume during the temperature decrease. The reverse transition into the anisotropic phase took place at about 333 K, which pointed to a considerable ($-70\ \text{K}$) overcooling compared to the point of the direct phase transition. On repeated heating, the picture of the process was totally reproducible. So the microscopic observations showed the following:

(1) evolution of absorbed solvent was possible in the temperature interval 333–354 K;

(2) phase transition into the isotropic phase was observed at about 409 K;

(3) phase volume of the cubic phase was probably dependent on temperature, which was connected to the changing state of the rotating molecules; and

(4) technological admixture was present in the initial crystals, amounting to 2–3% of the total mass.

4. Calorimetric Studies

Tris(hydroxymethyl)nitromethane crystals **1** were studied on a scanning Calvet-type microcalorimeter in the temperature range 293–390.5 K. During heating from 293 to 353 K for pressed polycrystals three peaks were observed: at $T_{KI}^{(1)} = 332$ K with $\Delta Q_I^{(1)} = -0.08$ kcal/mol, at $T_{KII}^{(1)} = 341$ K with $\Delta Q_{II}^{(1)} = -0.174$ cal/mol, and at $T_{KIII}^{(1)} = 352.5$ K with $\Delta Q_{III}^{(1)} = -5.80$ kcal/mol. The first one is probably connected to an outflow of solvent residue and the second to minor reconstruction of the crystal structure also linked with absorbed solvent evolution. No melting of the substance was registered in the interval 293–390.5 K. In some cases the main phase transition took place at $T_{KIV}^{(1)} = 355$ K with $\Delta Q_{IV}^{(1)} = -7.64$ kcal/mol. In the transition a distorted form of the peak and an uncertainty in temperature and ΔQ values were observed, which might be explained by two stage transitions linked with the probable influence of crystal lattice defects formed during pressing.

Tris(hydroxymethyl)aminomethane crystals **2** were examined with the same instrument in the range 293–467 K. The thermogram showed three peaks: the first, at $T_{KI}^{(2)} = 352$ K with a very small thermal effect, the second at $T_{KII}^{(2)} = 409$ K with $\Delta Q_{II}^{(2)} = -10$ kcal/mol, and the third one at $T_{KIII}^{(2)} = 433$ K with $\Delta Q_{III}^{(2)} = -1$ kcal/mol. Except for the very small third peak after the phase transition at $T_{KII}^{(2)}$ no thermal anomalies were found up to 467 K. It was probable that the third peak was connected to the melting, the thermal effect of which was 10 times smaller than $\Delta Q_{II}^{(2)}$.

5. IR Spectra

IR spectra of the crystals were recorded on a Specord 75 IR spectrophotometer in the range 400–4000 cm^{-1} at a spectral slit of no more than 3 cm^{-1} for the range 400–2000 cm^{-1} and 10 cm^{-1} for the range 2000–3700 cm^{-1} . Samples for IR spectroscopy were prepared by crushing the examined material in a mortar and subsequently pressing it in a mixture with KBr powder. For the crystal **1** in the temperature range 293–353 K the temperature behavior of symmetric stretching vibration absorption bands of nitro groups $\nu_S(\text{NO}_2)$ and stretching vibrations of hydroxyl groups $\nu(\text{OH})$ were examined. Both bands undergo strong changes during the temperature rise.

$\nu_S(\text{NO}_2)$ Behavior

In the region of symmetric stretching vibrations of the nitro group, $\nu_S(\text{NO}_2)$, IR spectra of the crystals **1** showed,

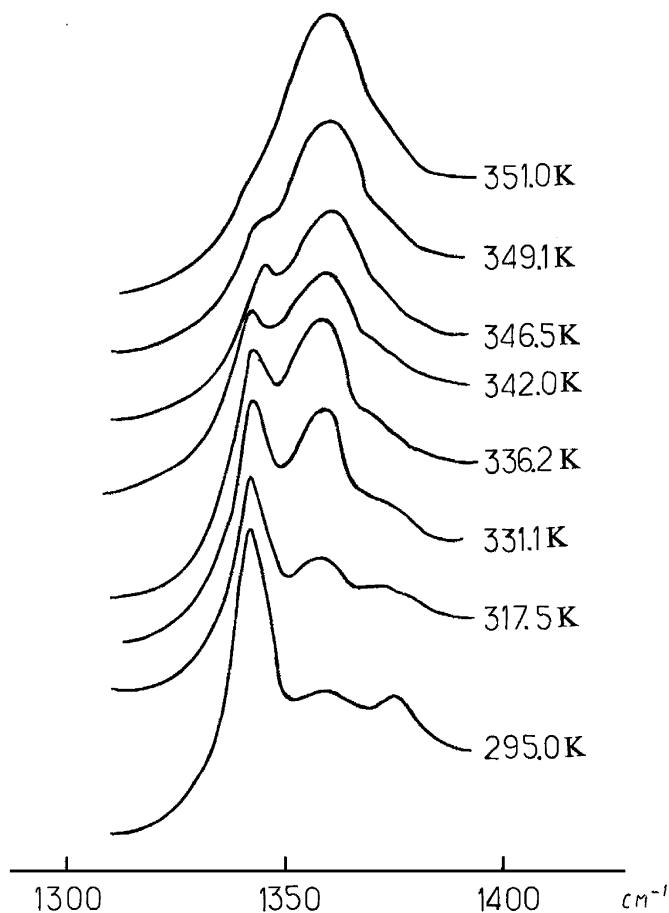


FIG. 5. Dependence of IR spectrum of the compound **1** in the region of symmetric valent vibrations of nitro groups on temperature.

as expected, two bands: an intensive one at ~ 1340 cm^{-1} and a broad one at ~ 1360 cm^{-1} . Taking into account the construction of two different molecules obtained from X-ray study, one can probably judge that the low-frequency band corresponds to the N(2)O(6)O(7) nitro group, which is more bound by orbital interaction with the C(6)O(8) bond, whereas the high-frequency band must correspond to stretching vibrations of the more mobile N(1)O(1)O(2) nitro group. In this case the additional broadening of the latter band can be explained by the force-field fluctuations. The intensity of the 1340- cm^{-1} band decreases and the 1360- cm^{-1} band increases with temperature growth (Fig. 5). No broadening of the $\nu_S(\text{NO}_2)$ band, which would be indicative of a fast ($\sim 10^{-11}$ s) reorientation with overcoming energy barrier, is observed. Instead, a gradual drop of the narrow $\nu_S(\text{NO}_2)$ band at ~ 1340 cm^{-1} and an intensity rise of the broad one, ~ 1360 cm^{-1} , take place. The width of the latter slightly depends on temperature, which indicates a fluctuational rather than rotation-relaxational mechanism.

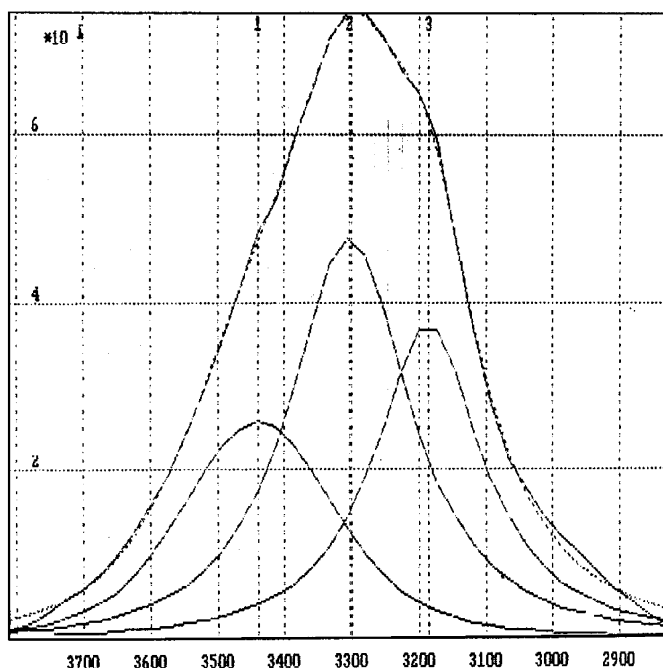


FIG. 6. Structure of the $\nu(\text{OH})$ band of the compound **1** at 294 K.

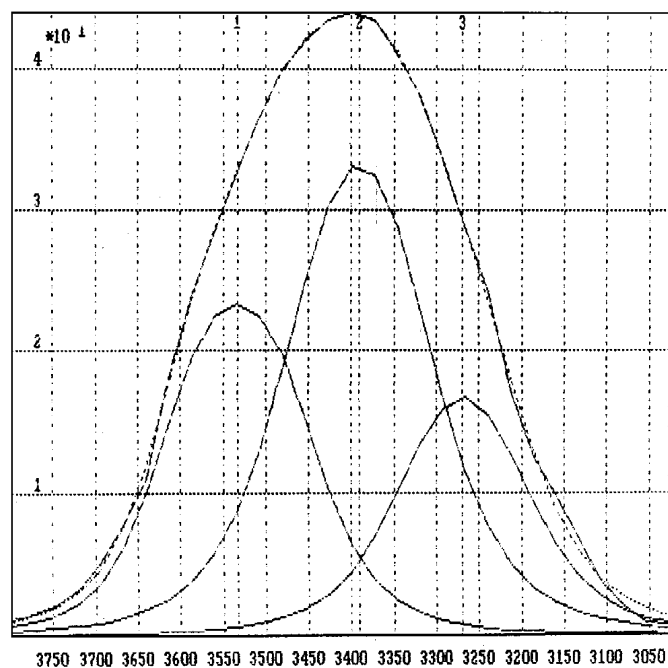


FIG. 8. Structure of the $\nu(\text{OH})$ band of the compound **1** at 356 K.

Behavior of O–H Stretching Vibrations

In the range of stretching vibration, IR spectra of the compound **1** at room temperature contain a complex band which splits into individual Voigt components at 3186.5, 3303, and 3439 cm^{-1} (Fig. 6). The splitting of the O–H

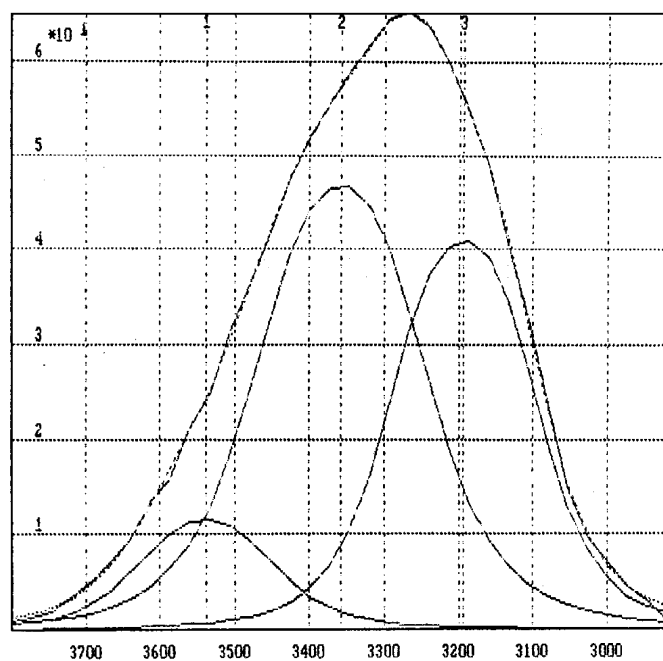


FIG. 7. Structure of $\nu(\text{OH})$ band of the compound **1** at 330 K.

stretching vibration contour was observed at enhanced temperatures too. At 330 K (Fig. 7) (long before phase transition) two weak H-bonds are replaced by two still weaker ones, the corresponding shifts of the bands being 3303 to 3358 cm^{-1} and 3439 to 3538 cm^{-1} . At the same time the most stable H-bond is still valid, only slightly weakening: 3186.5 to 3193.5 cm^{-1} .

At 356.8 K (after phase transition) (Fig. 8) the weak hydrogen bond remains, 3538 to 3532 cm^{-1} , and in this case the stable hydrogen bonds existing during prephase state are replaced by weaker H-bonds: 3193.5 to 3269.5 cm^{-1} and 3358 to 3391 cm^{-1} . Note that IR spectra of a low-concentration solution (0.03%) of the compound **1** in methylene chloride have the same set of hydrogen bonds, which the solid phase of compound **1** demonstrates at 356.8 K. So after the phase transition in the cubic phase only very weak intramolecular H-bonds along with weak intermolecular H-bonds exist.

The IR spectrum of the crystals **2** was recorded only at room temperature (Fig. 9). The broad band at $\sim 2500 \text{ cm}^{-1}$ can be assigned to a weak bond of a proton with the atoms of nitrogen and oxygen of the $\text{N}\cdots\text{H}^{\delta+}\cdots\text{O}$ type. The absorption band of O–H vibrations in the spectrum (Fig. 9) is masked by more intensive absorption bands of the NH_2 and $\text{NH}\cdots\text{O}$ vibrations. The IR spectrum of the low-concentration solution (0.03%) of the compound **2** in methylene chloride produces a picture where hydrogen bonds are completely absent and only a doublet of N–H stretching vibrations of free (non-hydrogen-bonded) NH_2 groups is present, which again masks the O–H vibrations.

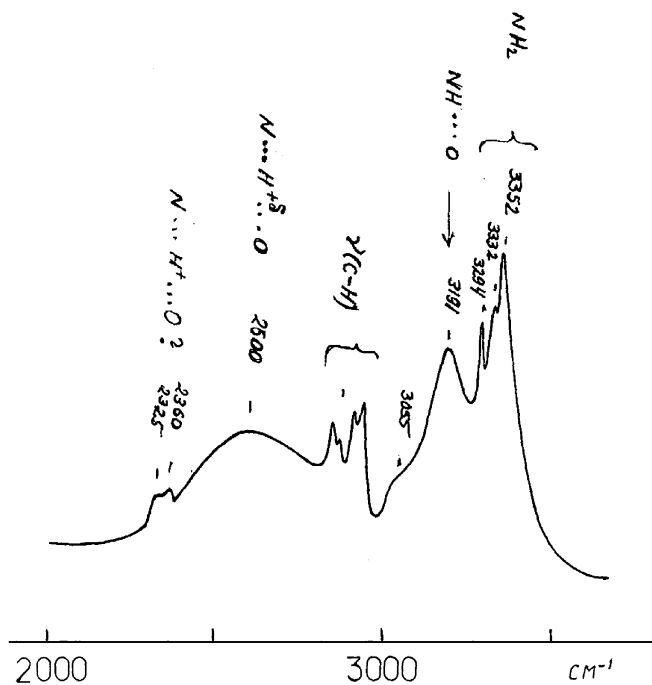


FIG. 9. IR spectrum of the compound **2** at 294 K.

It is important that the broad band at $\sim 2500\text{ cm}^{-1}$ responsible for weak "ionic" interactions of protons with nitrogen and oxygen atoms in the solid phase is totally absent in a diluted solution.

6. Temperature NMR Study in the Solid Phase

Relaxational free induction decay (FID) of protons was registered to examine the mobility of both the proton-containing fragments and the molecules as a whole, depending on temperature, using a pulse (RI-2303) spectrometer with a frequency of 60 MHz. The minimum temperature step was 5 K. The temperature accuracy was $\pm 1\text{ K}$. The measurement of the decay was done in an isothermic regime after reaching the necessary temperature and keeping it at the level for about 10 min. The temperature region of phase transitions was not recorded due to an instability of the process. In each case the temperature interval for investigation was chosen from the room temperature to the maximum possible one, which was limited either by melting and decomposition temperature of the substance or by technical possibility of the instrument. For the tris(hydroxymethyl)nitromethane crystals **1** the interval was from room temperature to 373 K (phase transition $\sim 353\text{ K}$) and for the tris(hydroxymethyl)aminomethane crystals **2** from room temperature to 413 K (phase transition $\sim 409\text{ K}$). The technical characteristics of the instrument prevented higher temperatures from being obtained. The method used is of low sensitivity for the

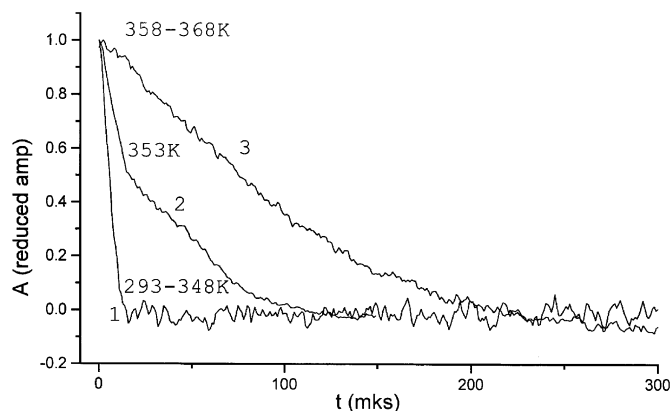


FIG. 10. Curves of the protons' signal decay (FID) in crystals of the compound **1** (293–348 K, the first group of curves; 353 K, the second group of curves; 358–368 K, the third group of curves).

proton signal decay change of motions having a barrier of less than 5–7 kcal/mol but it registers well the motions with barriers above this value. Therefore, if for the crystals of 2,2-dinitropropane-1,3-diol (**2**) the temperature dependence has been disclosed and the motion barrier value has been established ($\sim 15\text{ kcal/mol}$) so for the compounds **1** and **2**, we did not succeed in doing that because the value of the hydrogen bond energy (motion barrier) in the crystals is no more than 1.5 kcal/mol and imperceptible from the decay curves. Nevertheless, the data can produce important information as to the temperature dependence of the mobility of fragments and molecules. In both cases (Figs. 10 and 11) for crystals **1** and crystals **2** three groups of curves are isolated: the coinciding curves at the temperatures before phase transition (curve 1), the combined drop in the vicinity of phase transition (curve 2), and the slowly fading motion during rotation of the

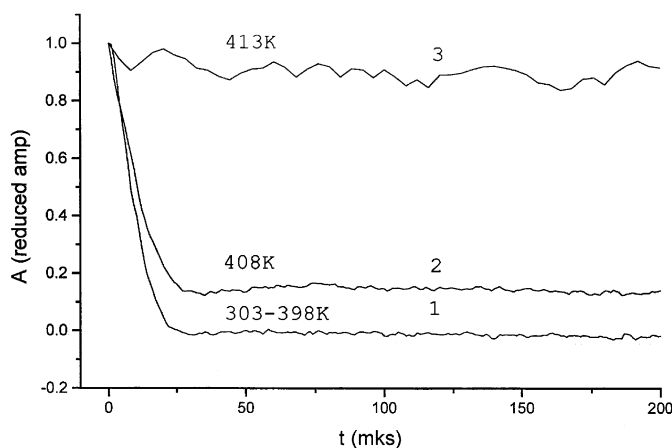


FIG. 11. Curves of the protons' signal decay (FID) in crystals of the compound **2** (303–398 K, the first group of curves; 408 K, the second group of curves; 413 K, the third group of curves).

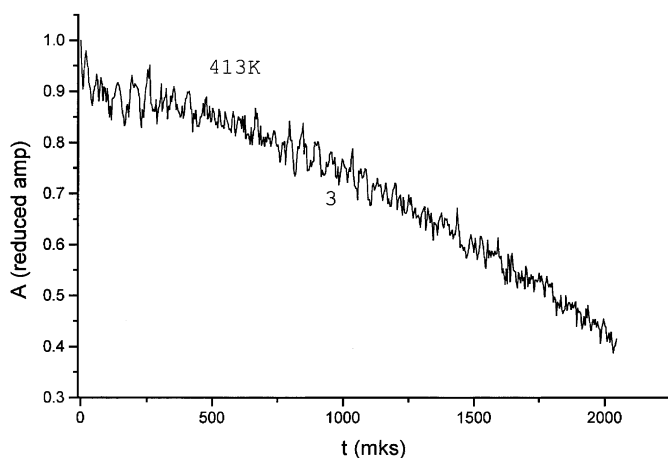


FIG. 12. Curves of the protons' signal decay (FID) in crystals of the compound **2** (413 K, the third group of curves, new time scale).

molecules as a whole in the temperature range above phase transition (curve 3). The decay in the phase transition region (curve 2) points out that a sudden liberation of all molecules of the substance does not take place and one part of molecules maintains its initial state while another part starts liberating (Fig. 10(2)). The fact is proved by the presence of both the sharp and the gradual drops of the signal at the same temperature. Curve 3 in Figs. 10 and 11 demonstrates the appearance of a noncomplicated motion; however, for crystals **1** the time of complete relaxation is not so considerable compared to that for crystals **2** (Fig. 12(3)), which points to the possibility of "hooking" between rotating molecules more for crystals **1** than for crystals **2**. So the NMR data corroborate the results of temperature behavior study of the mentioned compounds by other methods.

7. Proton Conductivity Measurement

Investigating physical properties of the compounds **1** and **2**, we concentrated on the following circumstances. During the calorimetric study of the tris(hydroxymethyl) aminomethane crystals **2** it was found that the thermal effect of the main phase transition from monoclinic phase to cubic phase constituted -10 kcal/mol and the melting heat of the cubic phase -1 kcal/mol; at the same time the total energy of the initial structure including van der Waals' and hydrogen bond energy amounted to -9.54 kcal/mol. The small deficit in the energy evidenced that some part of that was omitted. The second circumstance consisted of a broad absorption band in the region 2500 cm^{-1} found the IR spectrum of the solid phase of compound **2** which corresponded to a state of the proton having weak bonds with basic atoms of oxygen and nitrogen. The third circumstance was a crystallochemical one: with short contacts between oxygen atoms of

neighboring molecules ($2.5 < R < 2.75 \text{ \AA}$) the hydrogen atoms go out of the "hooking" between the two atoms and locate themselves above and below the contact of oxygen atoms. Such position of H atoms is not favorable to the formation of a strong hydrogen bond but probably facilitates proton exchange between them, which in turn must lower the crystal lattice energy and give a definite energetic gain. Taking into account the considerations, we ran experiments on proton conductivity measurements. The total conductivity of the compounds was measured by an impedance method on pressed tablets (pressure 20 MPa) with silver electrodes (tablet diameter 3 mm, thickness 1.4 mm). Impedance values were obtained using a VM-507 impedance meter (frequency interval 0.1–500 kHz). The conductivity calculation was done according to the technique (8). An electron component was found from the voltage–current response during direct current measurements. An ion component was determined as the difference of total and electron conductivity. The measurements for crystals **1** and **2** were conducted on symmetric cells $\text{Ag} \downarrow \text{substance} \downarrow \text{Ag}$. Crystals **1** had conductivity below the sensitivity of the instrument ($< 10^{-8} \Omega^{-1} \text{ cm}^{-1}$) during the temperature change from 293 to 348 K. At 348 K the conductivity increased to $4 \times 10^{-7} \Omega^{-1} \text{ cm}^{-1}$ and was, in general, of electron character. At 353–355 K the conductivity had a sharp rise to $2.6 \times 10^{-6} \Omega^{-1} \text{ cm}^{-1}$ (by five times for temperature change within 2 K). At the temperature to 391 K it gradually increased, reaching a value of $2 \times 10^{-5} \Omega^{-1} \text{ cm}^{-1}$, the activation energy of the process being equal to ~ 17 kcal/mol (Fig. 13a). The conductivity was of a combined electron–ion character and the electron component constituted nearly 30% of the total conductivity value. At the heating to 388 K the tablet did not undergo any noticeable change. The conductivity measurement in alternating current permitted both the electronic and ionic conductivity components to be

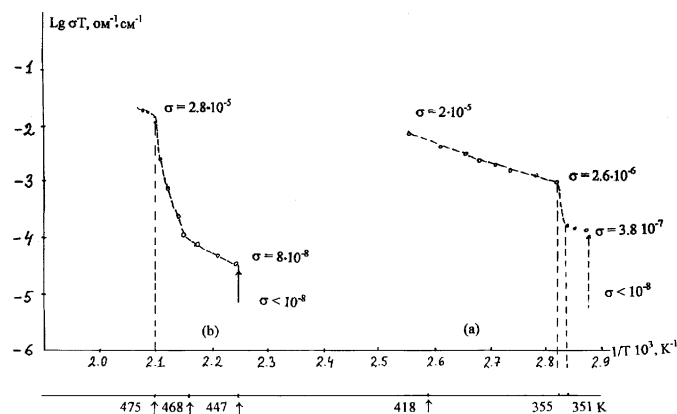


FIG. 13. Conductivity dependence on temperature in Arrhenius coordinates (a) crystals of the compound **1**, (b) crystals of the compound pentaerythritol).

obtained. Direct current measurement gives only the electron component of conductivity. It proved impossible to carry on the study of the conductivity temperature dependence for crystals **2** because the temperature interval between the main phase transition and the start of melting was small. Therefore, the measurements were carried out for separate temperature points. So at 293 K $\sigma_{\text{tot}} = 1 \times 10^{-8} \Omega^{-1} \text{cm}^{-1}$ and high resistance was maintained up to 413 K. At 415 K $\sigma_{\text{tot}} = 5.9 \times 10^{-6} \Omega^{-1} \text{cm}^{-1}$, at 419 K $\sigma_{\text{tot}} = 5.4 \times 10^{-5} \Omega^{-1} \text{cm}^{-1}$, at 422 K $\sigma_{\text{tot}} = 9 \times 10^{-5} \Omega^{-1} \text{cm}^{-1}$, and in this case the pure ionic component was equal to $\sigma_{\text{ion}} = 5 \times 10^{-5} \Omega^{-1} \text{cm}^{-1}$. At 424 K the electron component contribution dropped and the ion component was $\sigma_{\text{ion}} = 1.2 \times 10^{-4} \Omega^{-1} \text{cm}^{-1}$. After the experiment a tablet appeared to have reflowed. Despite the organic crystals having a narrow temperature interval of the cubic phase existence limited by phase transition below and melting above and a partial thermal decomposition of the substance being possible, the observed proton conductivity requires its explanation. The proton conductivity was also measured in the pentaerythritol crystals (Fig. 13b) in the molecule of which there are four hydroxymethyl groups. It was found that the compound demonstrates the presence of proton conductivity after the phase transition crystal \rightarrow plastic phase as well. From the start it was the conductivity of a mixed type, but then in the region of 475 K the ionic component sharply increased (electron component in this case had only 5%), and at 479 K the ion conductivity reached $\sigma_{\text{ion}} = 5 \times 10^{-5} \Omega^{-1} \text{cm}^{-1}$.

DISCUSSION

Complex studies of temperature-dependent structure-energy changes in the compounds having a poly(hydroxymethyl) grouping in a molecule were carried out. The molecules of the compounds have a low barrier of conformational transformations, which does not exceed 1.5 kcal/mol. The barrier value in the compound **1** molecules was calculated by quantum-chemical methods and an estimate of the barrier against the broadening of the $\nu_{\text{S}}(\text{NO}_2)$ band with temperature rise was also made. The broadening was found to be a fluctuational (non barrier) mechanism rather than a rotation-relaxational type. Due to such low barrier, the molecules in the crystal lattice can be presented in various forms with no strong difference between them. In such crystals long before (in terms of temperature) the main phase transition from the crystal to the plastic phase small conformational reorganizations of the molecules are possible, not disturbing the general symmetry of the crystal.

Calorimetric data on phase transitions and IR spectra of the stretching O–H vibrations can serve as evidence of the transformation. (Note that still before the phase transition a valent O–H vibration change takes place.) From IR

spectra that even at room temperature in crystals of the compounds very low energy of hydrogen bonds exists. The fact can be easily disclosed by a comparison of the frequencies of the valent O–H vibrations in the compounds of tris(hydroxymethyl)nitromethane **1** and 2,2-dinitropropane-1,3-diol (**2**) (in the compound **1** the frequencies are higher). The tendency of the intermolecular hydrogen bond energy drop is proved by calculations of the total energy of the lattice by the atom-atom potentials method. During the temperature lift the intermolecular hydrogen bond energy continues to decrease: in compound **1**, in the plastic cubic phase, the intermolecular hydrogen bond energy is insignificantly small. It resulted from our investigation (1, 2) that in the crystals of 2-bromo-2-nitropropane-1,3-diol with a low total energy of the crystal lattice the barrier of the conformational transition almost completely corresponded to the energy of structure-forming interactions, that is, to the hydrogen bond energy setting a definite architecture of the structure. In the presented case the energy of conformational transformations is very small; the energy of intermolecular hydrogen bonds is accordingly extremely small despite the molecules having tris(hydroxymethyl) grouping in their architecture. The low values of the intermolecular hydrogen bond are probably the main reason for the slowly fading motion during rotation of molecules as a whole in the temperature range above phase transition (NMR spectra). It may seem that the low value of the energy barrier during molecular rotation in the plastic phase provides such kind of molecular motion when the rotation frequency does not coincide with the frequency of proton exchange between neighboring molecules. Because of that, “free” protons can be traced in the intermolecular area. In such a way, probably, the occurrence of proton (ion) conductivity in the plastic phase can be explained for the investigated crystals. An important feature of the studied compounds is their ability to pass into the plastic state, the crystal structure of which is formed by rotating molecules. Regardless of numerous studies, the question of the structure of the compounds is far from being solved.

We did not succeed in making full X-ray study of separate crystals because of their temperature instability, and the basic information about the plastic crystal structure was obtained from temperature powder diffractograms. The basic reflections for crystal **1** are listed in Table 3. It resulted from the molecular package in the crystal that in the structure of the compound one could trace an image of a body-centered cubic lattice at room temperature. The same image could be found also in the powder diffractogram for the most pronounced reflections (Table 3, section A). After the transition into the plastic phase (Table 3, Section B), one could see that some reflection shifted in the direction of greater interplane distances. Complete isotropy of the material in polarized

light leads to the suggestion that in this case the plastic phase has the structure of a distorted body-centered cube (bcc). With further growth of temperature, the structure is maintained but some decrease of the cube parameter takes place, which indicates the possible diminution of the effective molecular volume because of weakening of the intermolecular and intensification of the intramolecular interaction (Table 3, section C). A powder diffractogram of the compound **2** at room temperature is shown in Table 4, section D. The well-pronounced image of the cubic structure is not seen in the diffractogram because of the presence of many strong reflections. The picture becomes different at the temperatures near the phase transition point (Table 4, section E). In this case the strongest reflections demonstrate the formation of a body-centered cubic structure with weak residual reflections of the parent phase. During a further temperature rise, the picture becomes complicated due to the appearance of new weak reflections (Table 5, section F) and the growth of their number (Table 5, section G). It is probable that systematic distortions of the crystal lattice appear to be connected with the change of the molecular rotation state and the appearance of the ion component in lattice interactions, which is corroborated both by IR spectroscopy data and by proton (ion) conductivity investigation. It should be noted that at these temperatures in polarized light a complete optical isotropy takes place, which to our mind confirms the retention of the distorted cubic structure. In both cases there are common reasons for producing the distortion of cubic structure. They can be a noncoincidence of mass centers and centers of the electron density of rotating molecules, a discordant precession of molecular dipoles during the rotation of molecules in the internal field of the crystal, and also the appearance of an ion component in intralattice interactions. The obtained data show that the complex experimental approach makes it possible to study temperature-dependent changes both in separate molecules and in the structure as a whole occurring in molecular crystals. In this case one can succeed in tracing the conformational changes of "hot" molecules accumulating the energy which could be

obtained in the molecules in some other way, for example, by mechanical deformation. Hence, further development of the work may follow, in connection with such questions as

(1) study of the influence of thermodynamic equilibrium (point) defects and dislocations in particular on conformational changes of the molecules located in the zone of their action,

(2) problems of aging and thermal decomposition (in particular, the investigation of causes of a phenomenon—retarding cell effect—the deceleration of the thermal decomposition rate in the solid phase compared to that in the liquid phase), and

(3) structure variations for just the same substance at different temperatures. Also, the appearance of proton conductivity in the plastic state attracts attention with the possibility of constructing proton (ion) conductors without the presence of water. All the questions mentioned above may be of interest for solid state chemistry.

ACKNOWLEDGMENTS

The authors are very grateful to L. O. Atovmyan for permanent interest in the work and to I. G. Gusakovskaya for the conducting of calorimetric measurements. The work was supported by the Russian Foundation for Basic Research (Grant 00-03-32885 a).

REFERENCES

1. N. I. Golovina, A. V. Raevskii, B. S. Fedorov, I. G. Gusakovskaya, R. F. Trofimova, and L. O. Atovmyan, *J. Solid State Chem.* **137**, 231–241 (1998).
2. N. I. Golovina, A. V. Raevskii, B. S. Fedorov, I. G. Gusakovskaya, R. F. Trofimova, N. V. Chukanov, S. A. Vozchikova, G. V. Shilov, V. P. Tarasov, L. N. Erofeev, and L. O. Atovmyan, *J. Solid State Chim.* **157**, 296–308 (2001).
3. N. I. Golovina, N. V. Chukanov, A. V. Raevskii, and L. O. Atovmyan, *Zh. Strukt. Khim.* **41**(2), 294–299 (2000).
4. D. S. Sake Gowda and R. Rudman, *J. Chem. Phys.* **77**(9), 4671–4677 (1982).
5. D. Eilerman and R. Rudman, *J. Chem. Phys.* **72**(10), 5656–5666 (1980).
6. M. F. C. Ladd, *Acta Crystallogr. B* **35**, 2375–2377 (1979).
7. J. Koo and N. L. Allinger, *J. Am. Chem. Soc.* **99**, 975–979 (1977).
8. N. G. Bukun, A. E. Ukshe, and U. F. Ukshe, *Elektrokhimiya* (29), 110 (1993).